

Supporting Information for “Lateral Variations Across the Southern San Andreas Fault Zone Revealed from Analysis of Traffic Signals at a Dense Seismic Array”

Hao Zhang¹, Haoran Meng² and Yehuda Ben-Zion^{1,3}

¹University of Southern California, Los Angeles, California, USA.

²Southern University of Science and Technology, Shenzhen, China.

³Southern California Earthquake Center, Los Angeles, California, USA.

Contents of this file:

1. Text S1
2. Figures S1 – S8
3. Table S1

Text S1: Particle motion analysis of waveforms

To clarify the character of observed signals, we first apply particle motion analysis using data from the event shown in Figure 2. We improve the SNR by shifting waveforms recorded by a 2D array on a BF using offsets determined by slowness solved with a method described in section 2.3. The aligned waveforms are then linearly stacked with equal weights. Figure S4 shows different components of the stacked waveform and particle motion diagrams within a 1-second window around reference zero time. The horizontal polarization is linear and aligns with wave propagation direction while vertical-radial particle motion follows a retrograde elliptical shape, indicating that the waveform is a Rayleigh wave. This analysis is repeated for additional events with various moving speeds and results show similar particle motion features (Figure S5).

Figure S1. (a) The spectrogram of vertical waveform recorded by node R1001 from 2020-03-07T17:15:00 to 2020-03-07T17:45:00. The vertical light blue stripes with energy from 2-35 Hz are traffic events on local road (Figure 1b). The horizontal strip with energy from 2-5 Hz, marked by the red rectangle, corresponds to a freight truck on the highway I-10. (b) The corresponding waveform bandpass filtered from 1 to 50 Hz. (c) The same waveform but bandpass filtered from 1 to 5 Hz. (d) The waveform of local car events (within the red rectangle in (b)) recorded by the linear array.

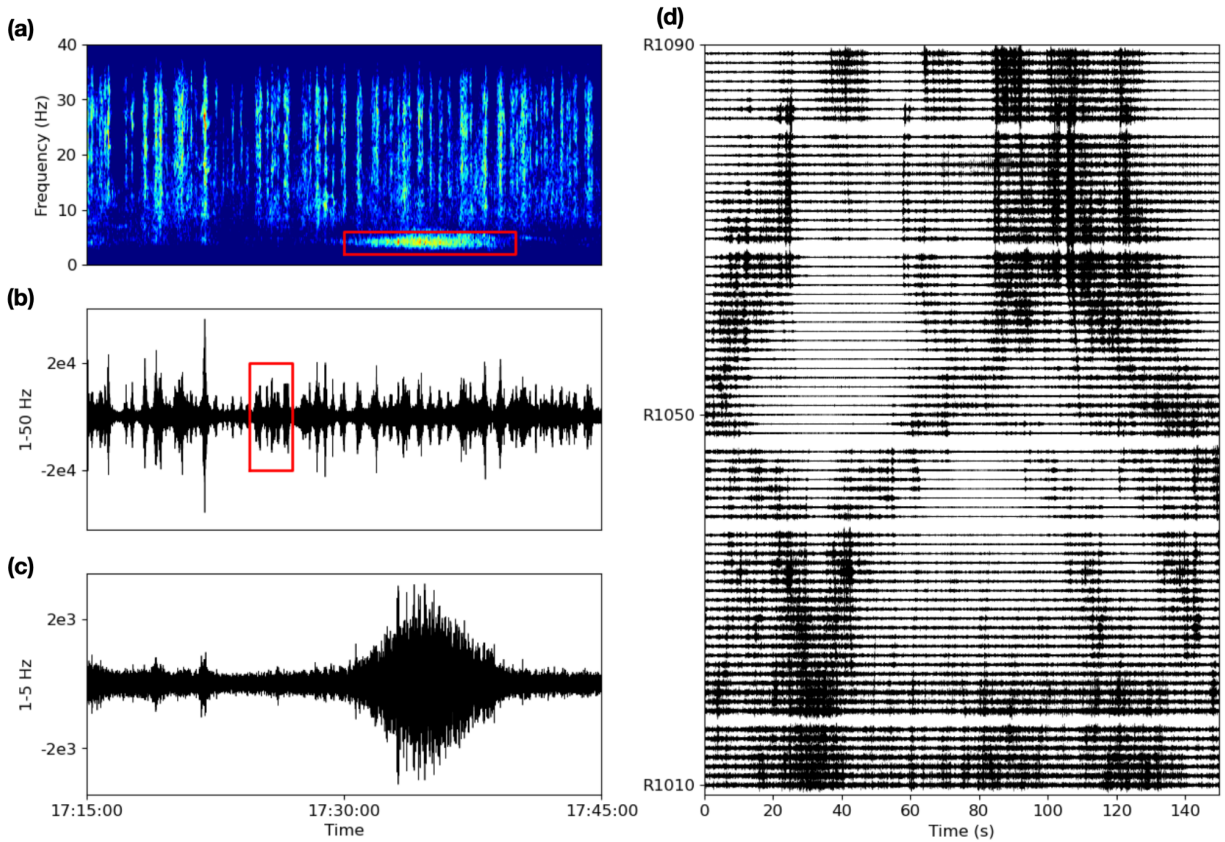


Figure S2. Tracking the moving vehicle source in event E1 using 2D arrays by resolving the propagation direction of Rayleigh wave. **(a,b)** Lag time distribution and wave propagation directions for the example time window in Figure 2a on the 2D subarrays centered on MCF and BF, respectively. Lag times are computed using waveform cross-correlations of a reference node and its neighbors. The Rayleigh wave propagation direction is determined by the opposite direction to the gradient of the lag times at the neighbors of all reference nodes at the center. **(c)** The location of the vehicle, denoted by the red star, is determined by the intersection of the railway and the wave propagation direction. The corresponding timing is determined by subtracting from the reference time the wave propagation time from source to node. The reference center of the railway denoted by the red dot is the closest point to the center of the subarray on BF. **(d)** The azimuth from the vehicle to the two subarrays on MCF and BF, and the distance from the vehicle to the center of the railway. The estimated speed of the traffic is 100 km/h.

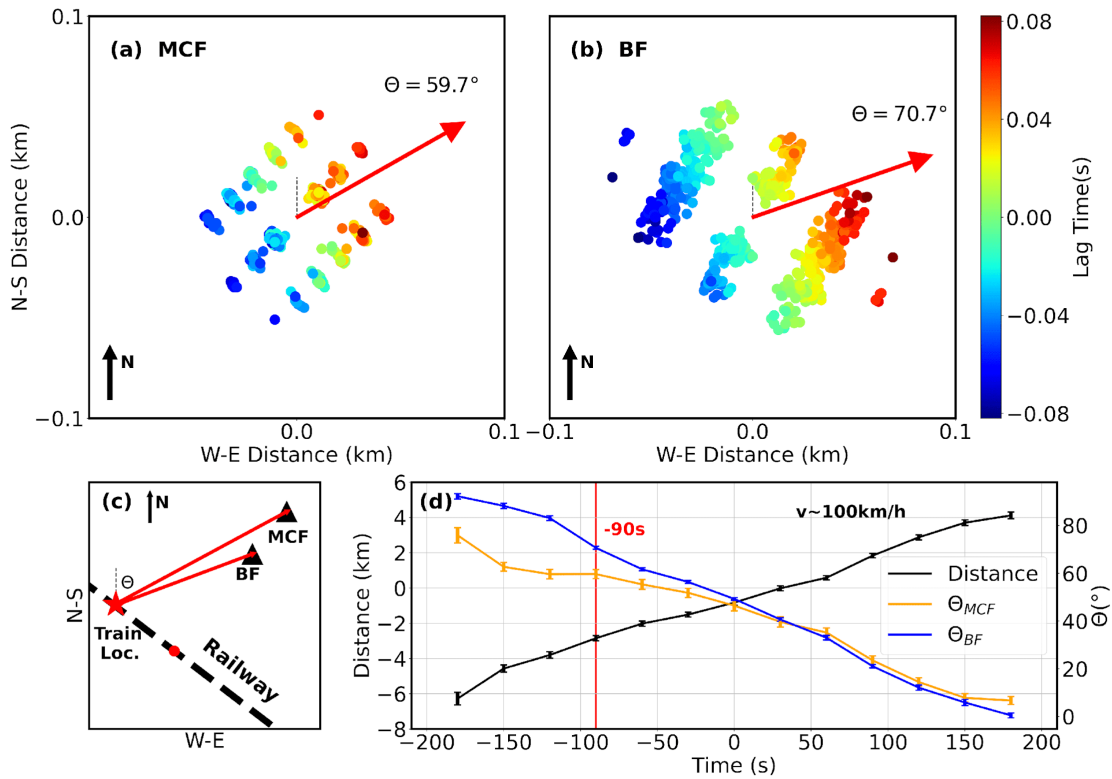


Figure S3. Sensitivity kernels of Rayleigh waves at 3 Hz (gray), 4 Hz (blue) and 5 Hz (red). The kernels are calculated using a 1D average version of the CVM-S4.26-M1 model in the study area, which includes a geotechnical layer representing seismic properties from surface to about 350m depth.

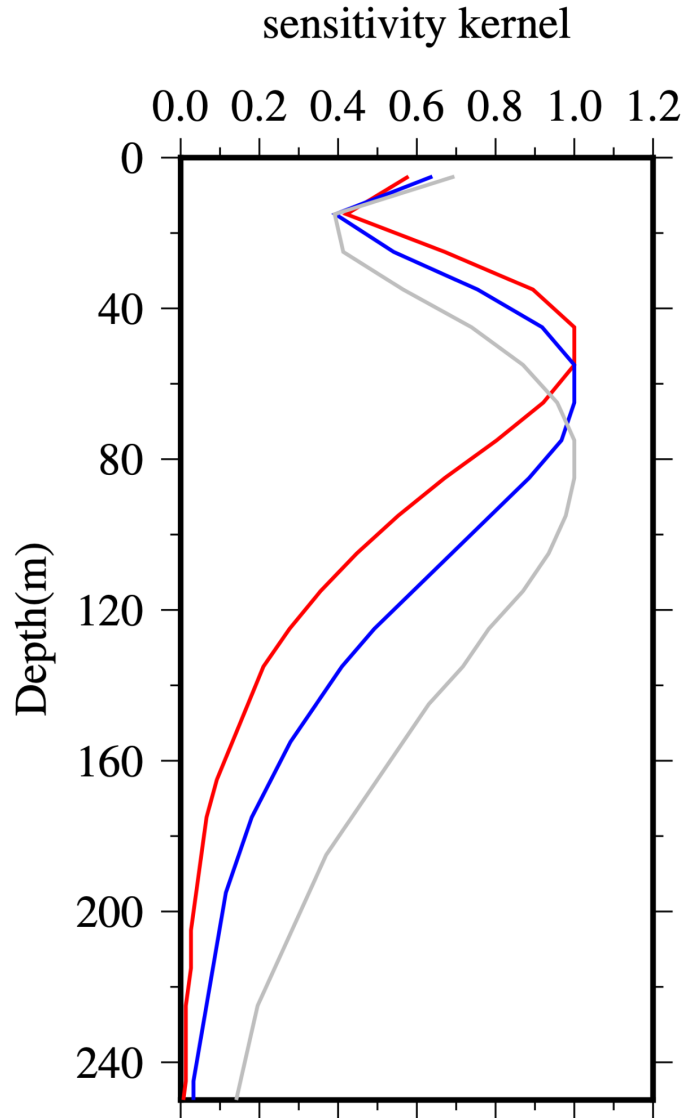


Figure S4. Particle motion analysis for the event in Figure 2 using the waveforms recorded by the 2D subarray in the frequency range 2-5 Hz. The waveforms are aligned and stacked to improve the SNR. The upper left and right panels show, respectively, the stacked waveforms in the vertical (Z), north-south (NS), east-west (EW), radial (R), and tangential (T) directions. The lower panels present particle motions for different pairs of components color-coded by time. The wave propagation direction is indicated by a red arrow in the horizontal particle motion diagram.

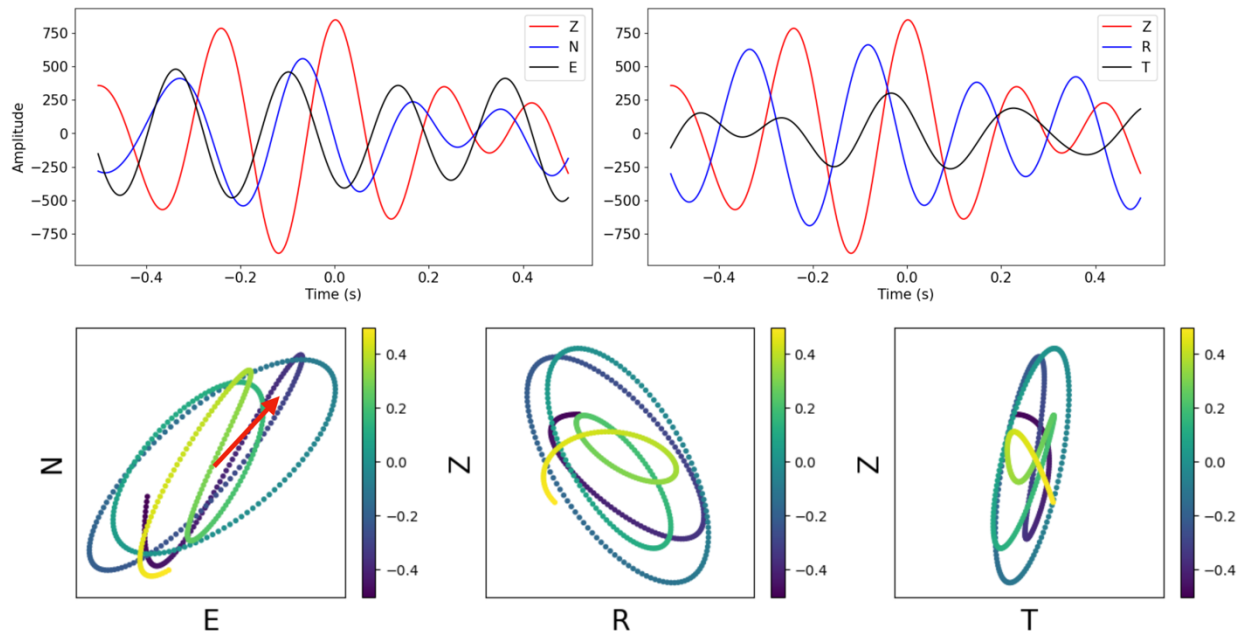


Figure S5. Particle motion analysis for Traffic event 20, similar to Figure S4.

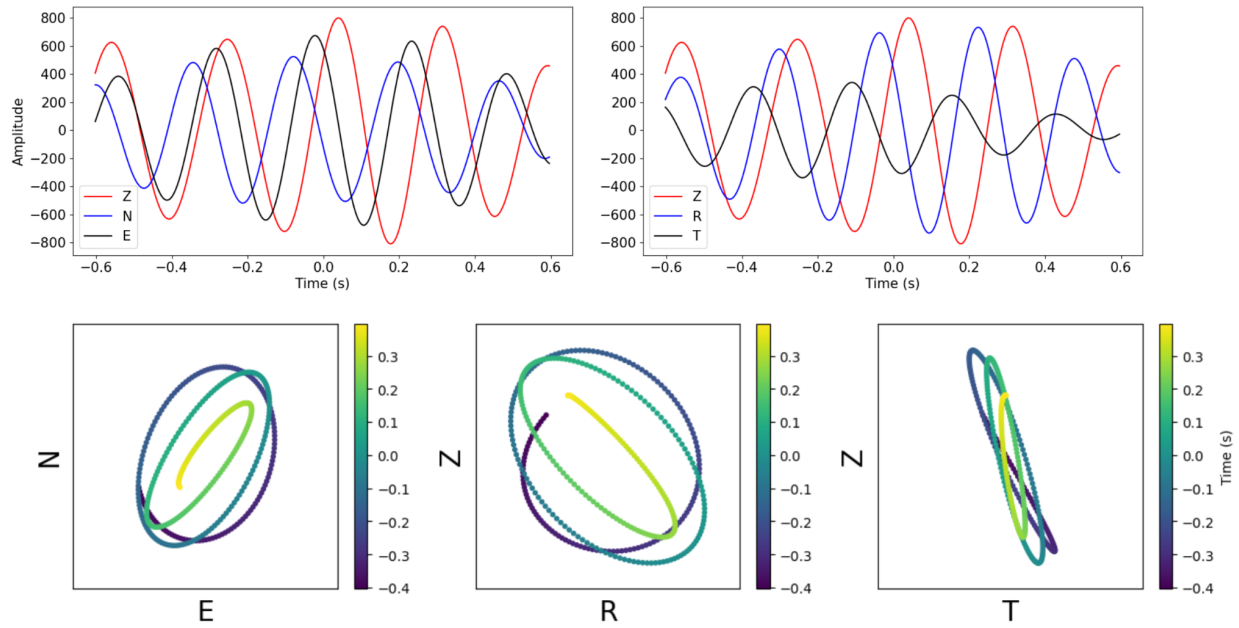


Figure S6. The distribution of speeds for the 29 analyzed traffic events. Fifteen signal sources have speeds lower than 85 km/h and are likely to be freight trains. The remaining fourteen events have speeds higher than 85 km/h and may be trucks on the highway.

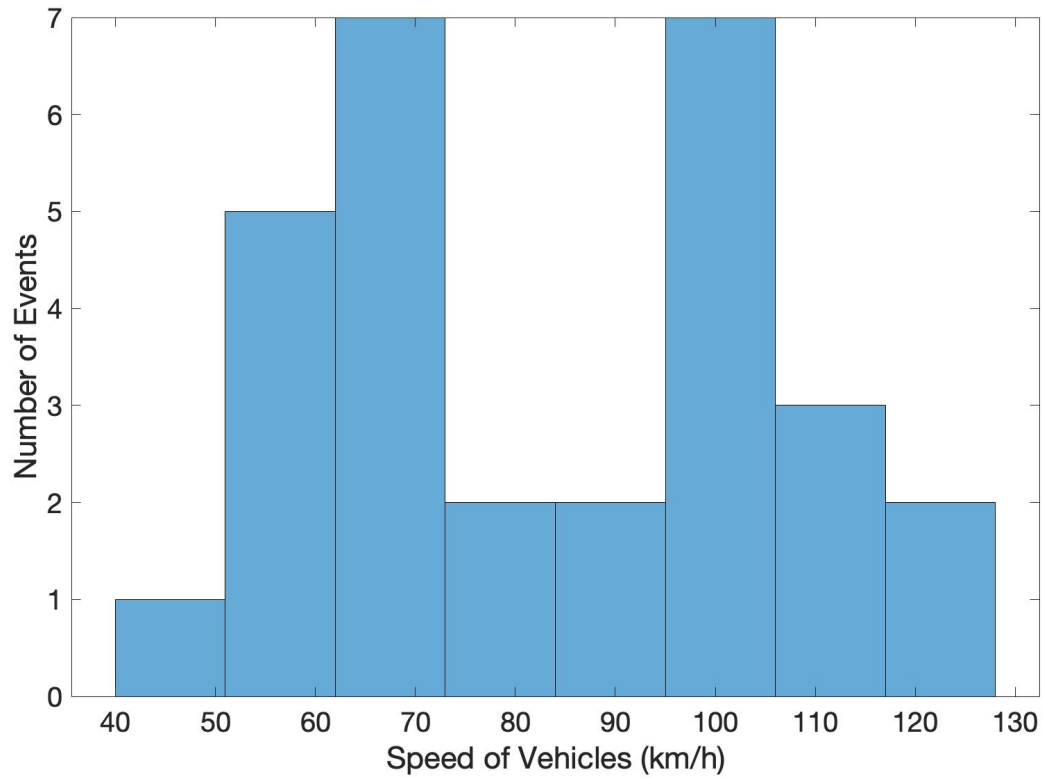


Figure S7. Rayleigh wave velocities resolved for different frequency bands. There is no clear dispersion observed in the frequency range of 2-5 Hz.

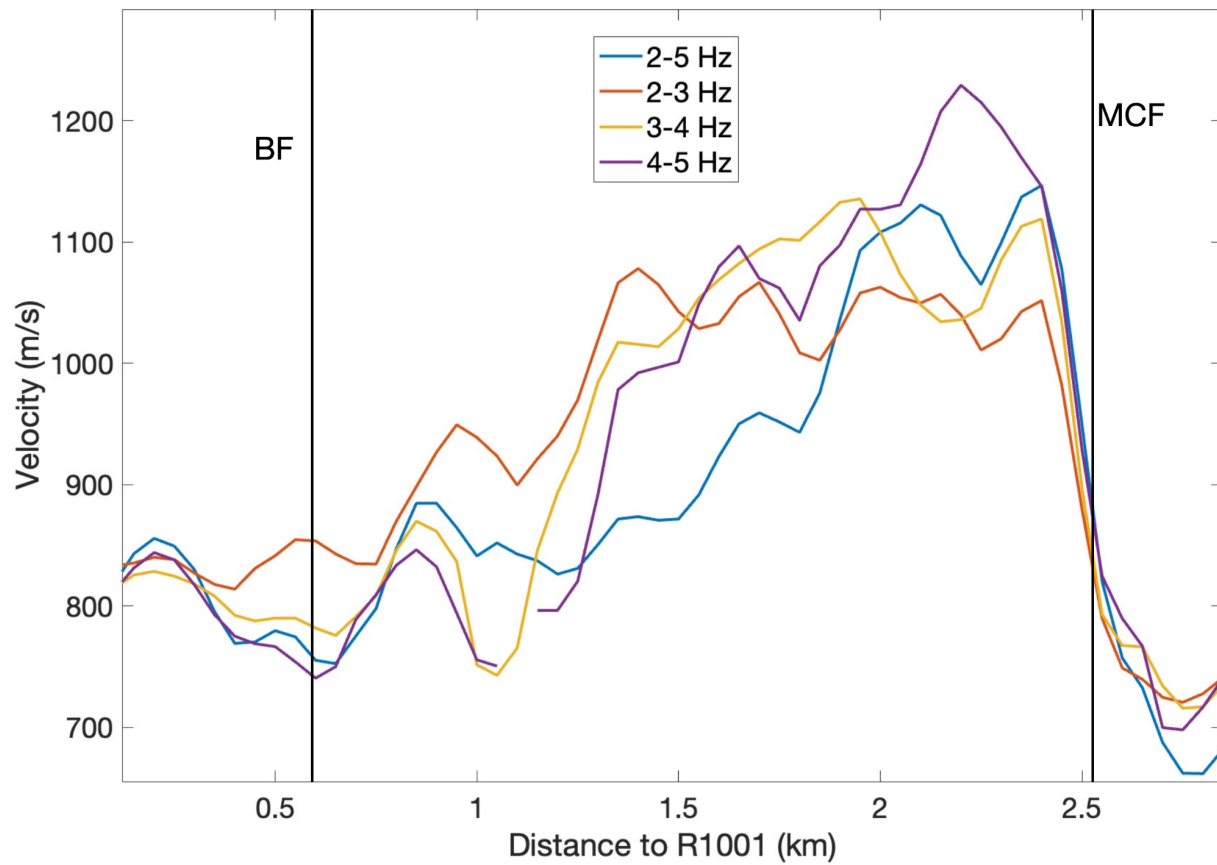


Figure S8. The RMS of signals at different nodes with (red curve) and without (black curve) correction of geometrical spreading. Each curve is normalized by the maximum RMS among all nodes.

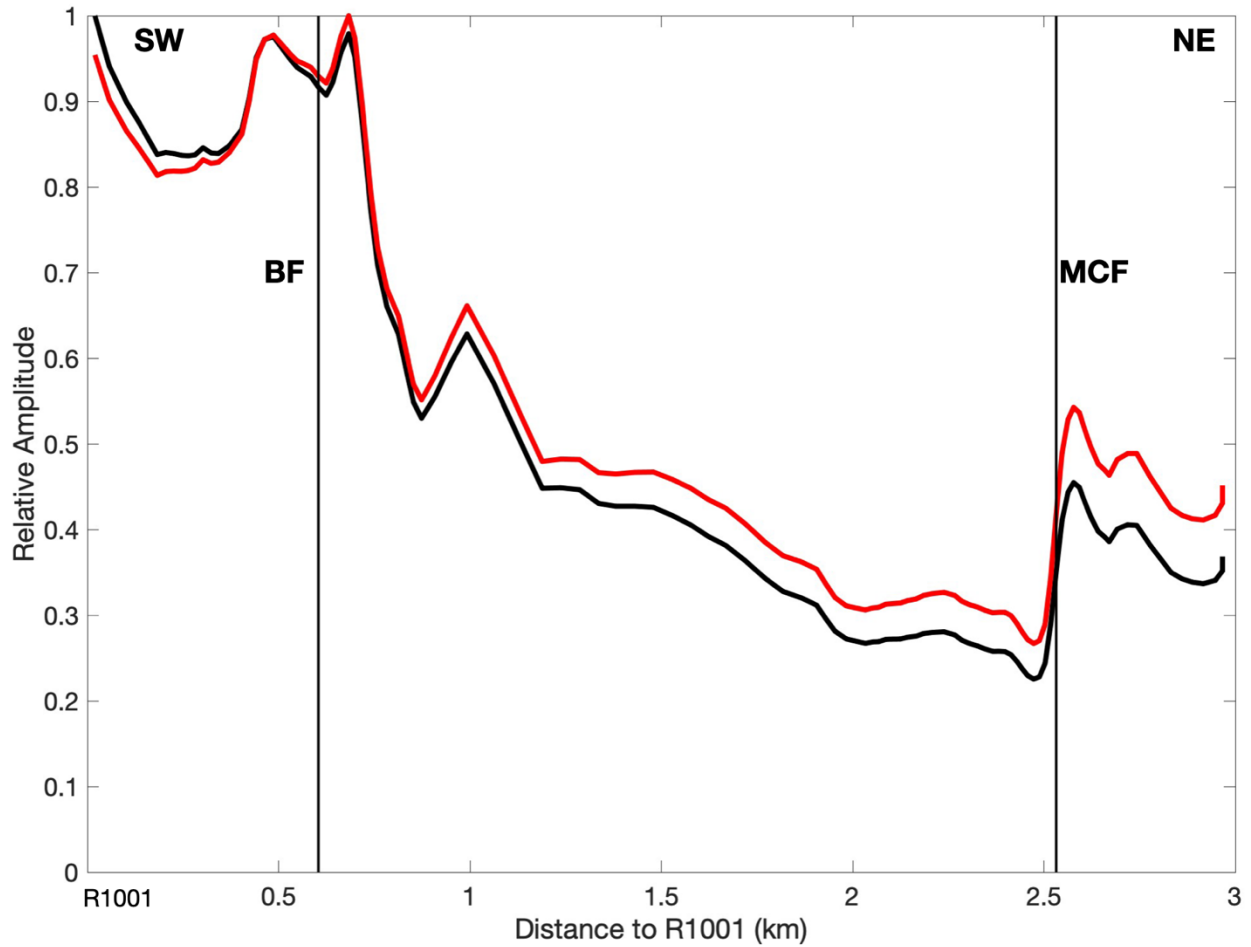


Table S1. Time and speed of 29 analyzed freight train or truck events on the railway or I-10.

Event Index	Time	Speed (km/h)
1	2020-03-06T11:00:30	61.14
2	2020-03-06T12:52:10	88.52
3	2020-03-06T13:56:40	72.56
4	2020-03-06T19:45:00	70.21
5	2020-03-06T20:42:30	94.78
6	2020-03-06T22:54:10	65.37
7	2020-03-07T00:19:10	96.01
8	2020-03-07T02:45:40	96.53
9	2020-03-07T08:31:40	65.82
10	2020-03-07T00:23:10	61.53
11	2020-03-07T09:53:00	56.96
12	2020-03-07T10:37:00	96.99
13	2020-03-07T14:46:40	82.23
14	2020-03-07T17:34:40	107.27
15	2020-03-07T19:51:20	100.74
16	2020-03-07T21:09:40	121.41
17	2020-03-08T02:37:30	61.23
18	2020-03-08T04:20:20	67.30
19	2020-03-08T07:05:30	104.54
20	2020-03-08T09:26:00	42.51
21	2020-03-08T10:43:50	67.36
22	2020-03-08T11:08:00	82.44
23	2020-03-08T11:30:00	96.49
24	2020-03-08T12:10:00	55.92
25	2020-03-08T15:53:20	105.54
26	2020-03-08T18:46:00	115.69
27	2020-03-08T20:20:00	116.91
28	2020-03-08T20:44:00	72.24
29	2020-03-08T22:45:20	113.90